Electronic Supplementary Material (ESI) for Journal of Materials Chemistry A.
This journal is © The Royal Society of Chemistry 2021

Electronic supplementary information

Electrocatalytic Fixation of N_2 into NO_3^-: Electron Transfer between Oxygen Vacancies and Loaded Au in Nb_2O_{5-x} Nanobelts to Promote Ambient Nitrogen Oxidation

Yintong Zhang[a], Feng Du[d], Ruyi Wang[a], Xintong Ling[a], Xiaoyong Wang[a], Qing Shen[f], Yujie Xiong[c], Tao Li*[b], Yong Zhou*[a,e], and Zhigang Zou[a,e]

[a] School of Physics, Eco-materials and Renewable Energy Research Center (ERERC), National Laboratory of Solid State Microstructures, Collaborative Innovation Center of Advanced Microstructures, Nanjing University, Nanjing, Jiangsu 210093, P. R. China.

[b] Engineering Technology Research Center of Henan Province for Solar Catalysis, School of Chemistry and Pharmaceutical Engineering, Nanyang Normal University, Nanyang, Henan, 473061, P. R. China.

[c] Hefei National Laboratory for Physical Sciences at the Microscale, Collaborative Innovation Center of Chemistry for Energy Materials (iChEM), School of Chemistry and Materials Science, University of Science and Technology of China, Hefei, Anhui 230026, P. R. China.

[d] Institute of Materials Science and Devices, School of materials science and Engineering, Suzhou University of Science and Technology, Suzhou, Jiangsu 215009, P. R. China.

[e] School of Science and Engineering, The Chinese University of Hong Kong (Shenzhen), Shenzhen, Guangzhou 518172, P. R. China.

[f] University of Electro Communication, Graduate School of Informatics and Engineering, 1-5-1 Chofugaoka, Chofu, Tokyo 1828585, Japan.

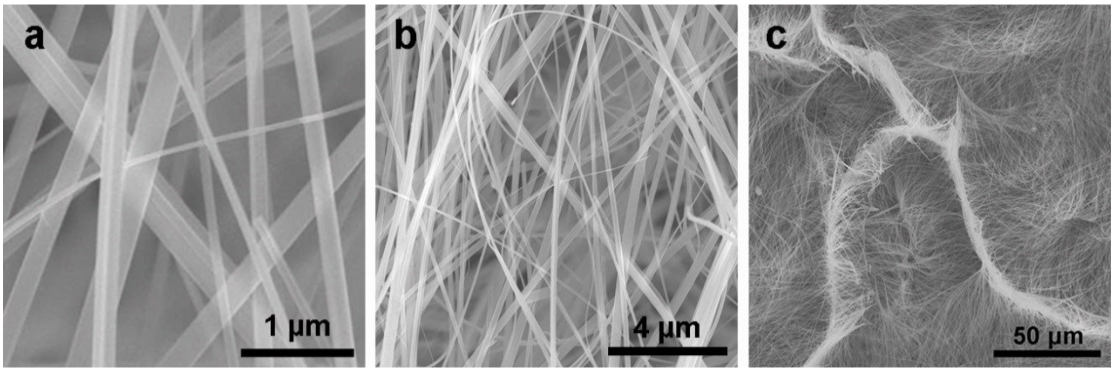

Fig. S1. SEM images of Nb_2O_5.

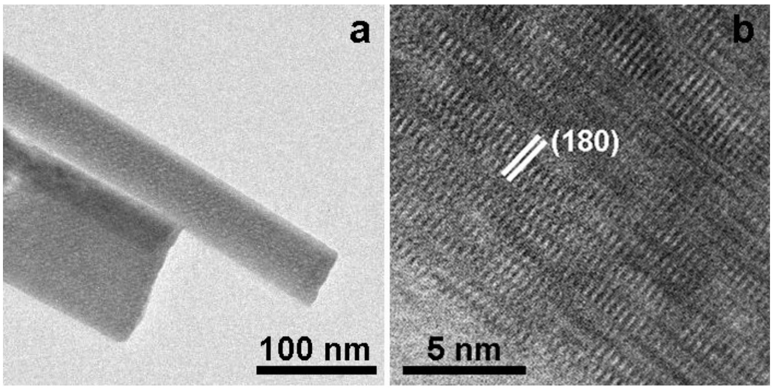

Fig. S2. (a) TEM image and (b) HRTEM image of Nb_2O_{5-x}.

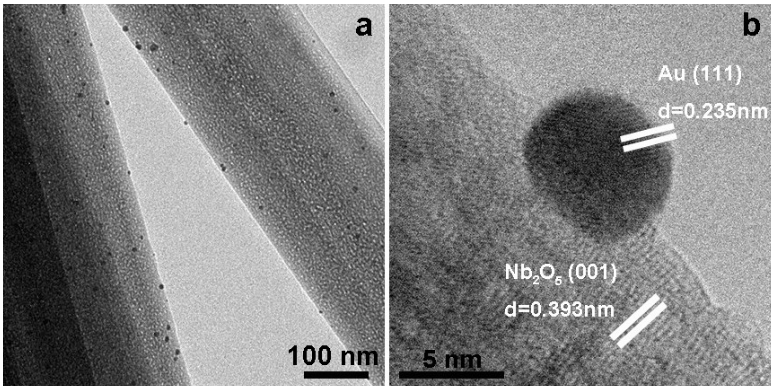

Fig. S3. (a) TEM image and (b) HRTEM image of Au-Nb_2O_5.

Table S1. Test results of ICP-MS.

	Mass of samples	**Volume of solution**	**Tested concentration of Au**
Au-Nb_2O_{5-x}	10.36 mg	250 mL	0.257 mg/L
Au-Nb_2O_5	8.52 mg	250 mL	0.201 mg/L

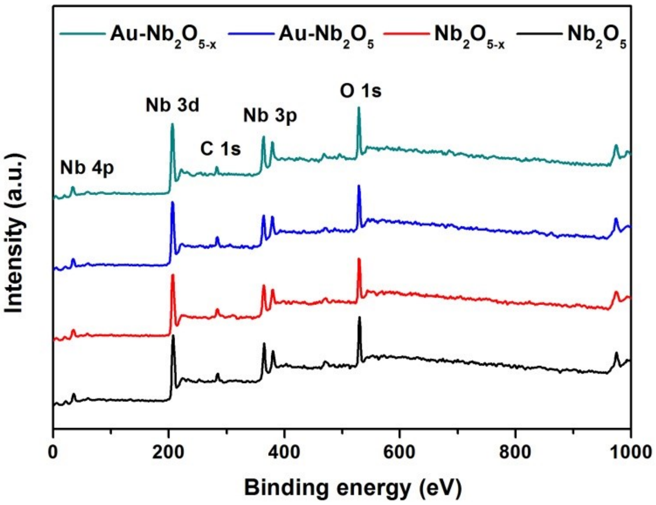

Fig. S4. XPS survey spectra of Nb_2O_5, Nb_2O_{5-x}, Au-Nb_2O_5 and Au-Nb_2O_{5-x}.

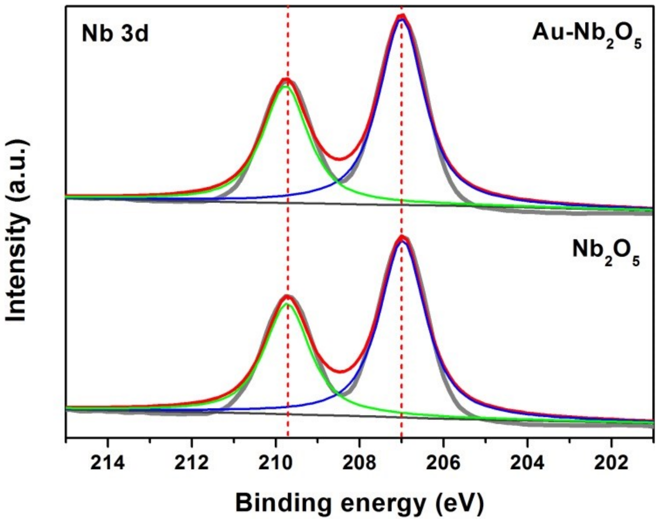

Fig. S5. XPS spectra of Nb 3d of Nb_2O_5 and Au-Nb_2O_5.

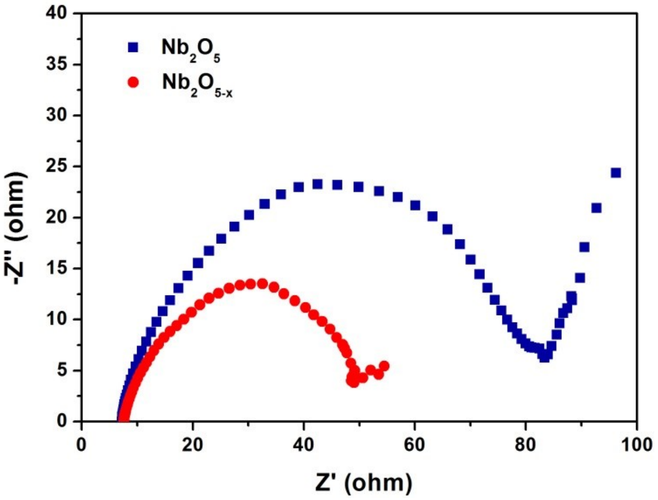

Fig. S6. EIS Nyquist plots of Nb_2O_5, Nb_2O_{5-x}.

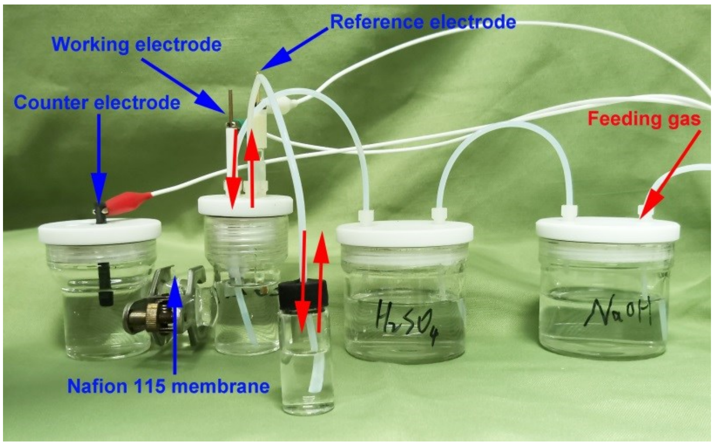

Fig. S7. Photograph of the reactor for NOR.

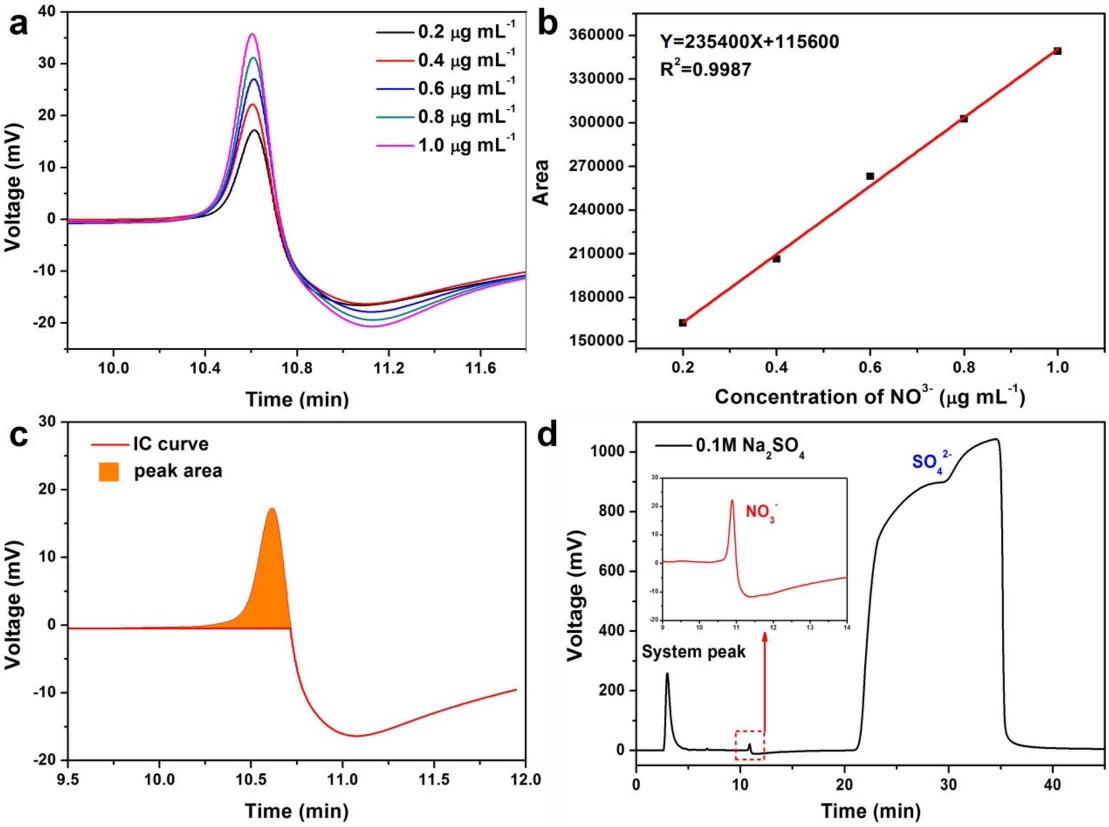

Fig. S8. (a) Ion chromatogram curves of a series of standard nitrate solution; (b) calibration curve of IC for nitrate concentration; (c) the range of peak area for nitrate in a typical IC curve; (d) IC curve for 0.1 M Na_2SO_4.

It is worth noting that there is a certain amount of nitrate in the applied commercial Na_2SO_4 electrolyte because of the impurities. The impurity contents fluctuate within a certain range in different batches of medicines, which may cause the difference in initial concentration of nitrate. Thus, in each NOR test, we detected both the initial concentration and the final concentration of nitrate in the anode electrolyte and calculated the net increasing amount which was adopted as the yield of nitrate. To ensure the reliability of our method, we did a series of experiment.

Fig. S9 a shows the initial and final IC curves of cathode electrolyte in a typical NOR test, which indicates the concentration of nitrate doesn't change, suggesting that Nafion 115 membranes can effectively prevent the transfer of nitrate between cathode and anode. Additionally, we put a piece of clean and unused Nafion 115 membrane into 0.1 M Na_2SO_4 solution in a beaker and another piece of Nafion 115 membrane which had been used for NOR test but without further treatment into another beaker with 0.1 M Na_2SO_4 solution as well. Both of them were soaked for 10 hours. The changes of the nitrate concentration in both solutions were detected and the results are shown in Fig. S9 b and c. The concentration in both solutions also didn't change, which indicates that the Nafion 115 membrane don't absorb or desorb nitrate in the electrolyte during the NOR test and affect the test results. Therefore, according to the above results, we confirm that the increment in the nitrate concentration of anode electrolyte can be adpoted to determine the NOR performance.

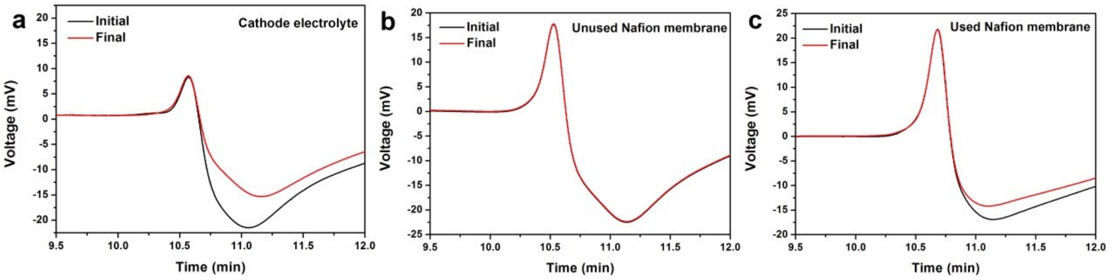

Fig. S9. (a) Initial and final IC curves of cathode electrolyte in a typical NOR performance test; initial and final IC curves of 0.1 M Na_2SO_4 solutions which were used to soak (b) unused Nafion membrane and (c) Nafion membrane after NOR test.

Table S2. The peak area of IC curves in Fig. S9.

Fig. S9 a	Peak area	Concentration increment
Initial	59996	~0
Final	60933	
Fig. S9 b	Peak area	Concentration increment
Initial	170600	~0
Final	171580	
Fig. S9 c	Peak area	Concentration increment
Initial	216564	~0
Final	217339	

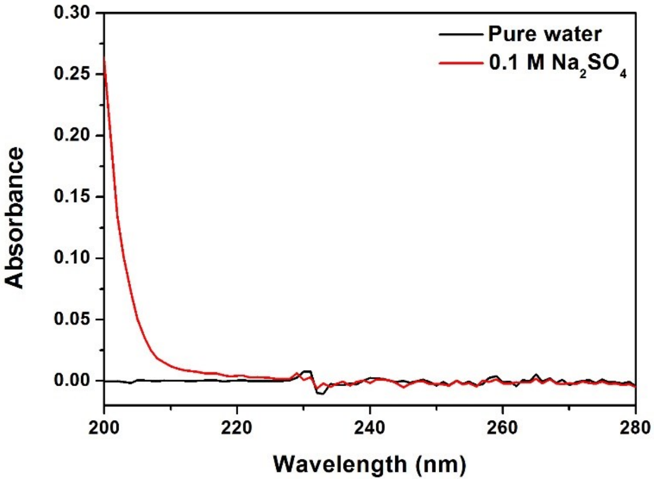

Fig. S10. UV absorption spectra of pure water and 0.1 M Na_2SO_4 solution.

It is worth noting that there is a certain amount of nitrate in the applied commercial Na_2SO_4 electrolyte because of the impurities, which is consistent with the results of IC data. Thus, to eliminate the effects of the impurities, we used 0.1 M Na_2SO_4 solution as the baseline for all the UV tests.

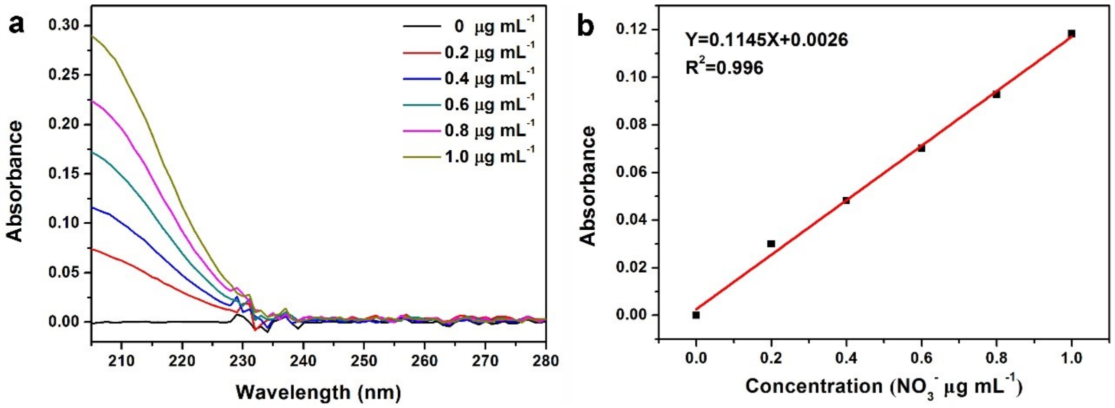

Fig. S11. (a) UV absorption spectra of a series of standard nitrate solution in 0.1 M Na_2SO_4; (b) calibration curve of UV absorption for nitrate concentration.

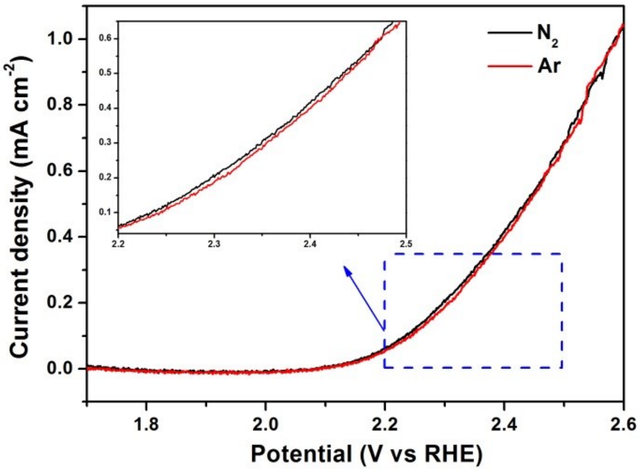

Fig. S12. LSV curves of Au-Nb_2O_{5-x} at a scan rate of 5mV s^{-1} in Ar- and N_2-saturated 0.1 M Na_2SO_4 solution.

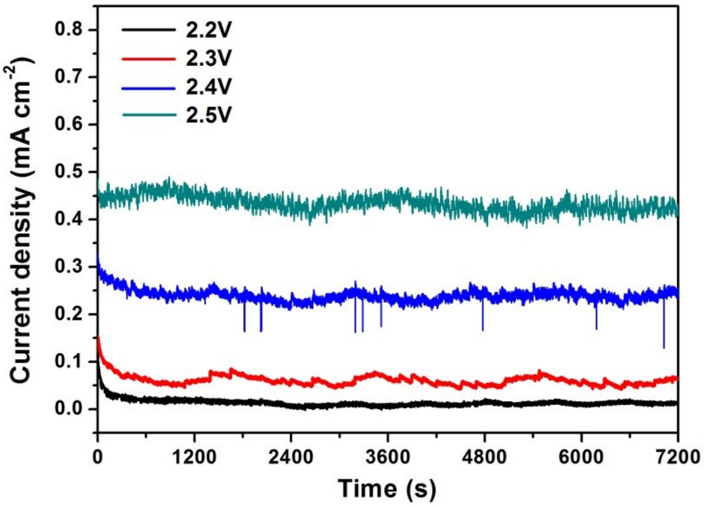

Fig. S13. Chronoamperometry curves of Au-Nb_2O_{5-x} at different applied potentials in 0.1 M Na_2SO_4 solution for NOR performance test.

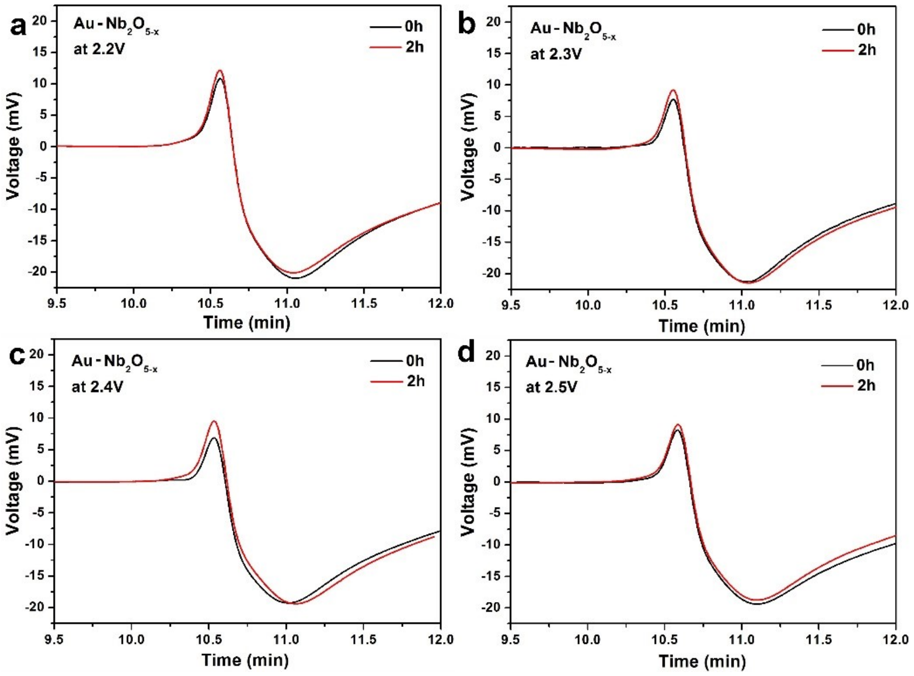

Fig. S14. Initial and final IC curves of Au-Nb_2O_{5-x} for NOR performance test at (a) 2.2 V, (b) 2.3 V, (c) 2.4 V and (d) 2.5 V.

Table S3. The peak area of IC curves in Fig. S12 and the calculated concentration increments of nitrate in each test.

Potential	2.2V		2.3V	
	Peak area	Concentration increment	Peak area	Concentration increment
0h	94922	0.0598	53362	0.098
2h	109026		76576	
	2.4V		2.5V	
	Peak area	Concentration increment	Peak area	Concentration increment
0h	50441	0.1527	69820	0.041
2h	86394		79473	

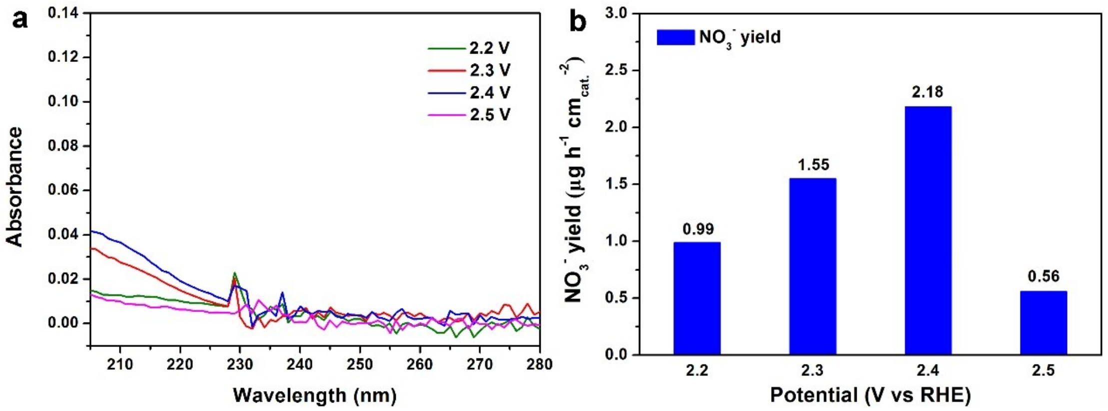

Fig. S15. (a) UV adsorption spectra of the electrolyte after NOR performance test for Au-Nb_2O_{5-x} at different potentials; (b) the calculated yield rates of Au-Nb_2O_{5-x} at different potentials by UV method.

Table S4. The peak area of IC curves and the corresponding concentration of nitrate for time-dependent NOR test of Au-Nb_2O_{5-x}.

Operational time	Peak area	Concentration
0h	144887	0.1445
2h	187295	0.3048
4h	214310	0.4196
6h	239338	0.5259

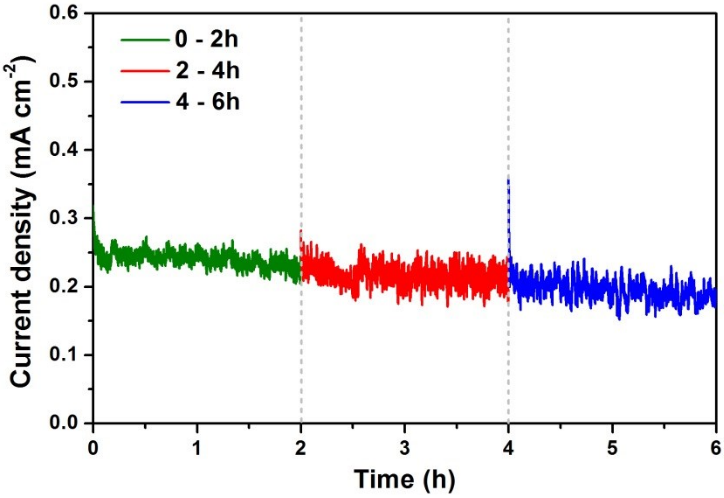

Fig. S16. Chronoamperometry curves of time-dependent NOR test of Au-Nb_2O_{5-x} at 2.4 V.

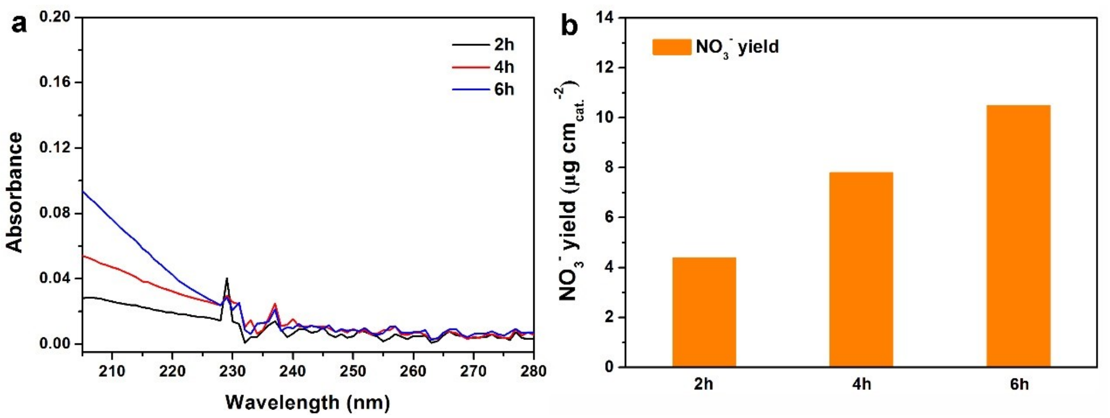

Fig. S17. (a) UV adsorption spectra of the electrolyte for the time-dependent NOR test of Au-Nb_2O_{5-x} at 2.4V; (b) the calculated yield rates by UV method.

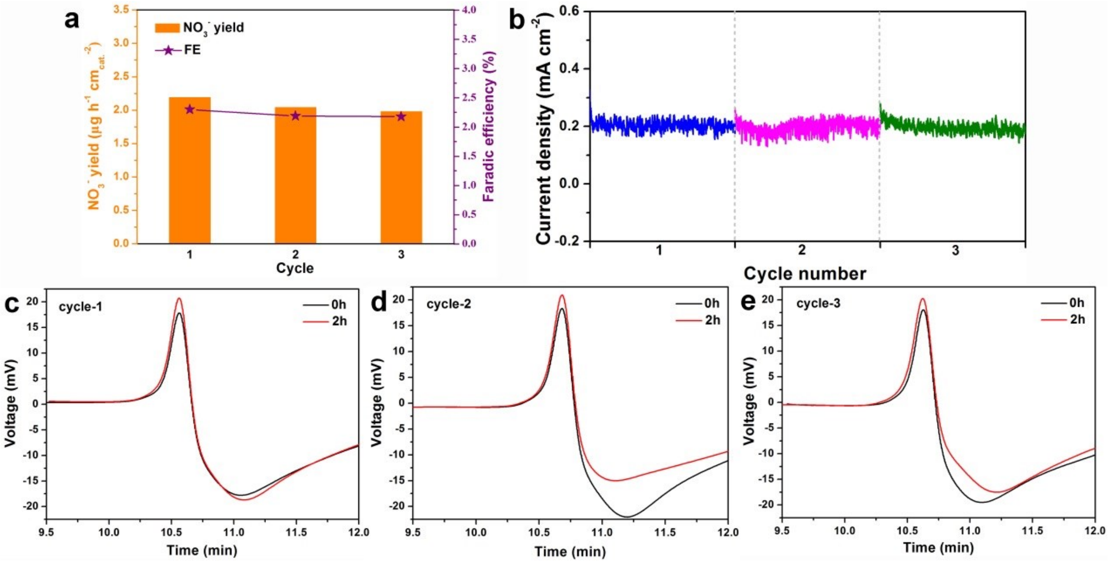

Fig. S18. (a) Nitrate yield rates and FEs and (b) chronoamperometry curves of Au-Nb_2O_{5-x} for NOR cycling test at 2.4 V; (c)-(e) initial and final IC curves of electrotyle for each cycle of Au-Nb_2O_{5-x} NOR cycling test at 2.4 V.

Table S5. The peak area of IC curves in Fig. S14 and the calculated concentration increments of nitrate in each cycle test.

Cycle-1	Peak area	Concentration increment
0h	154722	0.1469
2h	189302	
Cycle-2	Peak area	Concentration increment
0h	184386	0.1367
2h	216564	
Cycle-3	Peak area	Concentration increment
0h	179576	0.133
2h	210884	

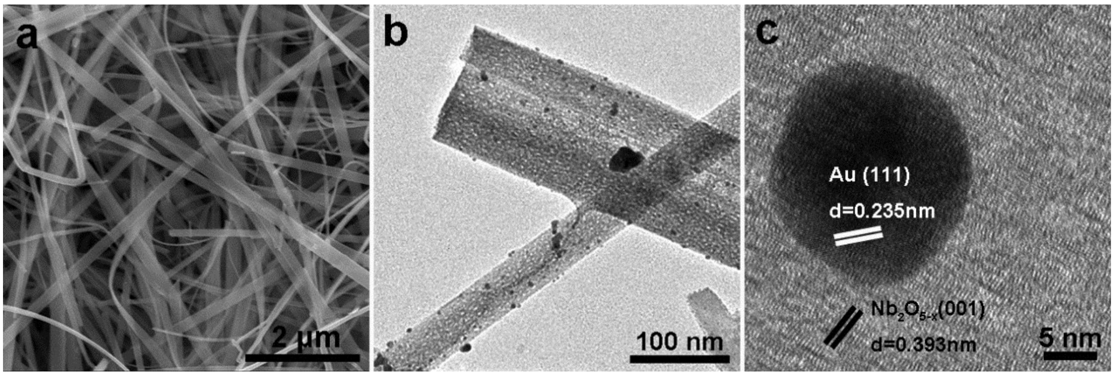

Fig. S19. (a) SEM image, (b) TEM image and (c) HRTEM image of Au-Nb_2O_{5-x} after cycling NOR test at 2.4 V.

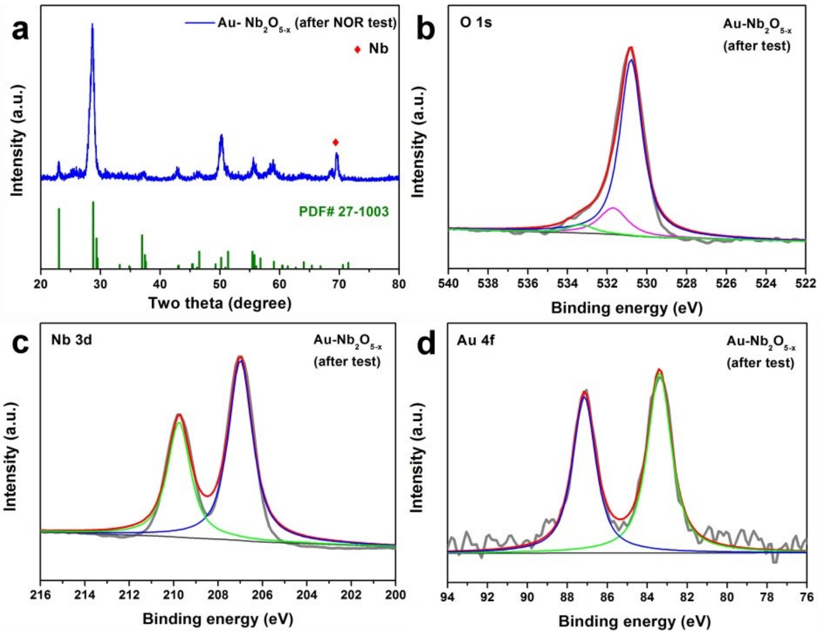

Fig. S20. (a) XRD pattern and XPS spectra of (b) O 1s, (c) Nb 3d and (d) Au 4f of Au-Nb_2O_{5-x} after cycling NOR test at 2.4 V.

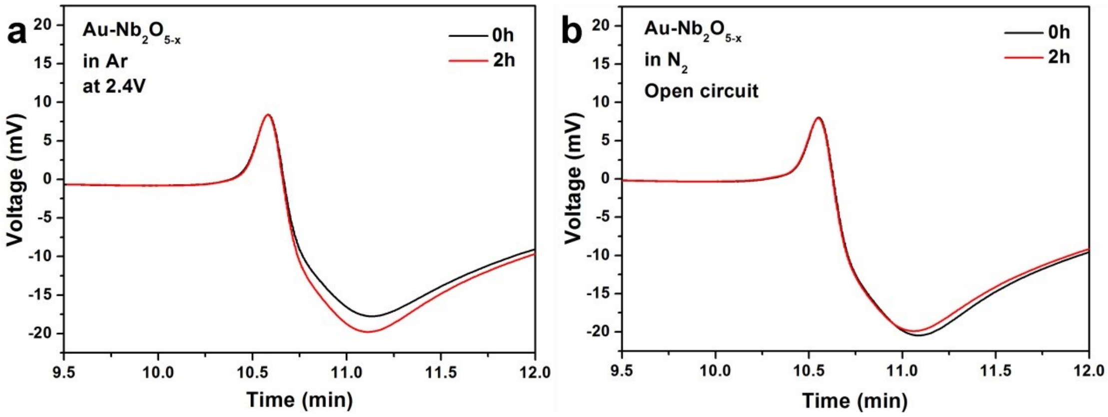

Fig. S21. Initial and final IC curves of electrotyle for control experiments of Au-Nb_2O_{5-x} (a) in Ar at 2.4 V and (b) in N_2 with an open circuit.

Table S6. The peak area of IC curves in Fig. S17 and the calculated concentration increments of nitrate in electrolyte.

In Ar	Peak area	Concentration increment
0h	81034	~0
2h	80797	
In N_2 with an open circuit	Peak area	Concentration increment
0h	70309	~0
2h	70588	

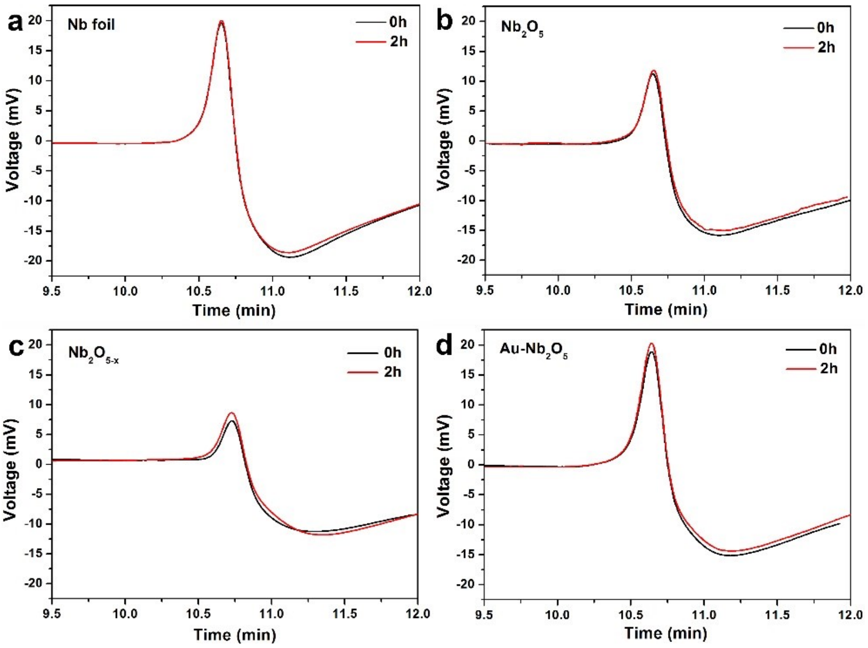

Fig. S22. Initial and final IC curves of (a) Nb foil, (b) Nb_2O_5, (c) Nb_2O_{5-x} and (d) Au-Nb_2O_5 for NOR performance test at 2.4 V.

Table S7. The peak area of IC curves in Fig. S18 and the calculated concentration increments of nitrate in electrolyte.

	Au-Nb_2O_5		Nb_2O_{5-x}	
	Peak area	Concentration increment	Peak area	Concentration increment
0h	190112	0.0606	56459	0.0704
2h	204377		73037	
	Nb_2O_5		Nb foil	
	Peak area	Concentration increment	Peak area	Concentration increment
0h	101575	0.024	185398	0.0068
2h	107223		186998	

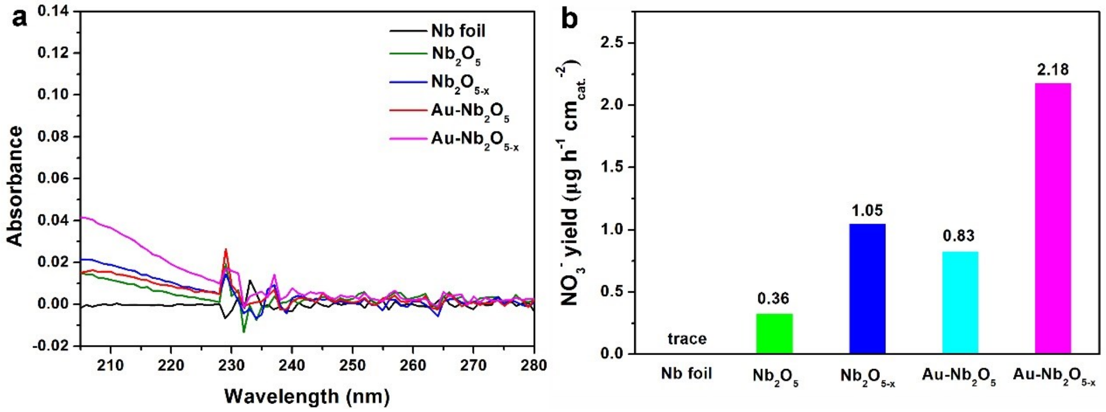

Fig. S23. (a) UV adsorption spectra of the electrolyte for NOR test of comparison samples at 2.4V; (b) the calculated nitrate yield rates of comparison samples by UV method.

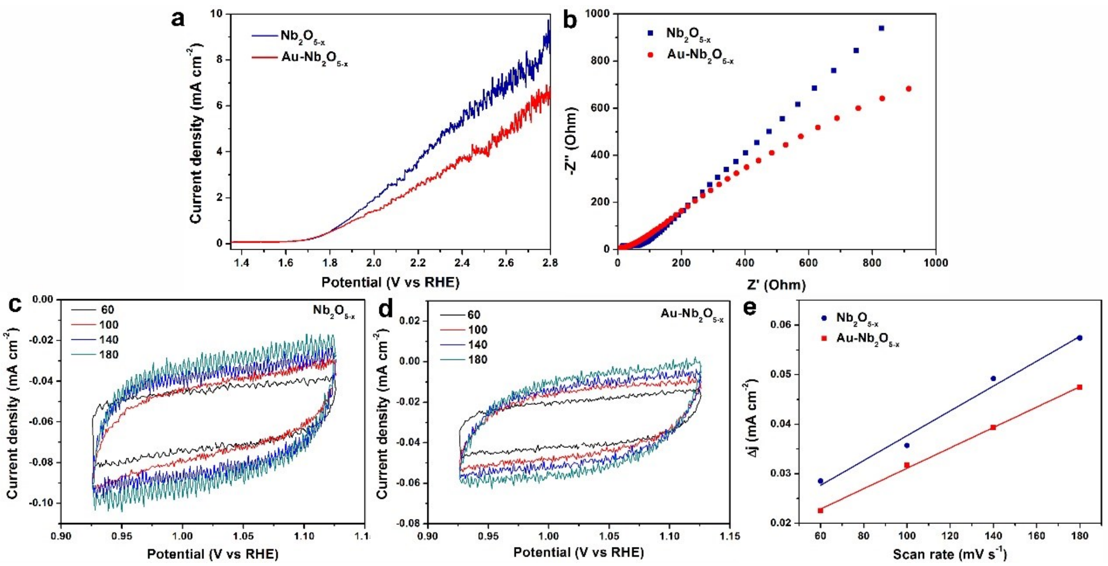

Fig. S24. (a) LSV curves and (b) Nyquist plots of Nb_2O_{5-x} and $Au-Nb_2O_{5-x}$ in Ar-saturated 1.0 M KOH solution; cyclic voltammograms of (c) Nb_2O_{5-x} and (d) $Au-Nb_2O_{5-x}$ in Ar-saturated 1.0 M KOH solution at different scan rates from 60 to 180 mV s^{-1}; (e) dependence of capacitive current density on scan rates of Nb_2O_{5-x} and $Au-Nb_2O_{5-x}$.

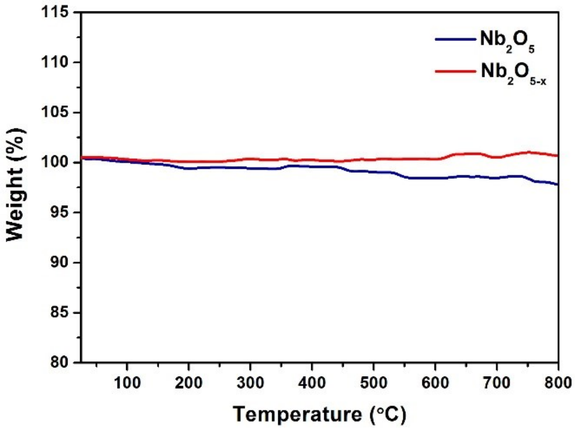

Fig. S25. Thermogravimetric curves of Nb_2O_5 and Nb_2O_{5-x} under N_2 atmosphere.

As shown in Fig. S25, the thermogravimetric analysis experiment was carried out under N_2 atmosphere. During the temperature increasing from room temperature to 800°C, the mass loss of Nb_2O_5 occurred due to its deoxidation, while the mass of Nb_2O_{5-x} remains unchanged. These results can explain the source of the strong TPD signal of Nb_2O_5.